SEMARAK ILMU PUBLISHING

Journal of Advanced Research in Fluid Mechanics and Thermal Sciences

Journal homepage:
https://semarakilmu.com.my/journals/index.php/fluid_mechanics_thermal_sciences/index
ISSN: 2289-7879

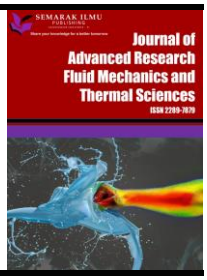

Heat Transfer and Entropy Generation of Turbulent Flow in Corrugated Channel using Nanofluid

Karima Heguehoug Benkara-Mostefa[1,*], Rahima Benchabi-Lanani[1]

[1] Applied Energetics and Pollution Laboratory (LAEP), Mechanical's Engineering Department, University of Mentouri Brothers Constantine 1. Ain El Bey Road, 25000 Algeria

ARTICLE INFO

Article history:
Received 25 June 2023
Received in revised form 28 August 2023
Accepted 11 September 2023
Available online 28 September 2023

Keywords:
Corrugated channel; entropy; finite volume method; generation; nanofluids turbulent flow

ABSTRACT

This paper presents a numerical study of two-dimensional, turbulent flow with heat transfer in a corrugated channel using 3% of Al_2O_3 nanoparticles volume fraction dispersed in a basic fluid (water) with a particle diameter of 30nm. The equations governing the flow are: the energy equation to model heat transfer, the momentum equations and the continuity equation. To simulate different values of the Reynolds number ranging from 1000 to 6000, the CFD code Ansys- Fluent based on the finite volume method is used. For turbulence modeling, the k-ε realizable model was used. The results are validated by other scientific work. Nu, skin friction coefficient, pressure drop and PEC factor are explored. We noted that the increase in the Reynolds number leads to an increase in the average Nusselt and a decrease in the coefficient of friction. Particular attention is paid to the generation of transfer entropy, friction and general entropy as well as the Bejan number. The transfer entropy generated in the fluid crossing the channel as well as the Bejan number decrease with the increase of the Reynolds while that of the friction increases. In addition, the use of nanofluid (Al_2O_3/water) gives better heat transfer than pure water.

1. Introduction

The improvement of heat exchanges in many industrial sectors requires the intensification of heat transfers by convection, to do this, a large number of researchers have carried out several numerical and experimental tests to increase the exchange surface, others, have worked on heat transfer fluids, and the essential parameter which makes it possible to evaluate the potential heat exchange is the thermal conductivity. The idea is then, to disperse nanoparticles in a basic fluid in order to increase its conductivity, hence the birth of the nanofluids. A turbulent forced convection of nanofluids flow for Reynolds number (1000<Re <5000) is explored in triangular-corrugated channels, Varieties nanoparticles have been considered (ZnO, SiO_2, CuO and Al_2O_3) with different diameters and volume fractions respectively from 30 to 70 nm, and from 0% to 4% [1]. The authors concluded that the decrease in the diameter of the nanoparticles and the increase in their volume fraction generate an

* *Corresponding author.*
E-mail address: benkarak@gmail.com

https://doi.org/10.37934/arfmts.109.2.136150

increase in the pressure drop, the heat transfer and the average Nu. In addition, the (SiO_2-water) is the nanofluid that offers the highest thermal-hydraulic performance than other types of nanofluids, while pure water has the lowest improvement in heat transfer. In Manca *et al.,* [2], a numerical study concerning the forced convection of turbulent flow with nanofluid (Al_2O_3-Water), with volume fractions between 0% and 4%, in a two-dimensional channel with different shapes (square and rectangular), is carried out. The Re is taken between 20,000 and 60,000. The results show that as well as the Re and the volume concentration of the nanoparticles increases, there is an improvement in the heat transfer accompanied by an increase in the pumping power. In Chen *et al.,* [3], the authors investigated numerically and experimentally the heat transfer performance and turbulent flow characteristics in smooth and asymmetric corrugated tubes. The results show that the thickness of the thermal boundary layer on the tube side is greater than that on the shell side, where the turbulent kinetic energy intensity is obviously higher. For $Re < 45000$, the $PEC > 1$. Moreover, the corrugated tubes can significantly improve the overall heat transfer coefficient by 10 to 20% compared to the smooth tube. Ajeel *et al.,* [4] were interested in numerical and an experimental study of different shapes of corrugated channels using different volume fractions of Al_2O_3 nanoparticles, $\Phi = 0\%, 1\%$ and 2% in order to improve the heat transfer for Reynolds numbers varying from 10000 to 30000. The results reveal that the trapezoidal corrugated shape is recommended experimentally and numerically, moreover, the increase in Re and volume fractions causes an increase in Nu and pressure drop of the nanoparticles for all shapes. An entropy generation study of nanofluid flow in porous media through different cases of sinusoidal corrugated channel in order to determine the optimal geometry is carried out. The considered flow is laminar and the used model is that of Darcy – Brinkman – Forchheimer. For the validation of the numerical procedure, the obtained results were compared to the corresponding numerical data. They reveal that the increase in the Darcy number leads to the increase of the thermal entropy and the reduction of the entropy of friction. In addition, when increasing the volume fraction of the nanoparticles (Al_2O_3 and CuO), an increase in the average Nusselt number and friction factor compared to a decrease in the coefficient of performance (PEC) were observed [5]. In Yang and Yang [6], the study is devoted to numerical simulation of fully developed turbulent flow with constant heat flux imposed in a circular tube. The temperature and flux fields were simulated by CFD, but the rate of entropy generation was calculated in post-processing. The two turbulence models (k–ε realizable and SST k–w) and analytical correlations were used as reference to prove the accuracy of the (SST k–w–ϕ–α) model used to predict the rate of entropy generation in complex systems. The results reveal that the Prt (turbulent Prandtl number) impacts the entropy transfer: the best results are obtained for the (SST k–w–ϕ–α) and (k–ε realizable) models for $Pr_t = 0.85$; however, for $Pr_t = 0.92$ and the (SST k–w) model, the optimal result is obtained. As regards the friction entropy, the results are the same for the two models (k–ε realizable and SST k–w), but for the (SST k–w–ϕ–α) model, a difference of 14% is detected for a Reynolds number of 100,000, which requires the integration of a method that uses the effective eddy viscosity. Also, the properties of the fluid according to the temperature must be considered when the radical change of this one is imposed. A 2D numerical study of the air flow through corrugated channels with sharp edges, where particular attention was paid to the effect of the variation of the Reynolds number and the aspect ratio (pitch / length) on the entropy generation, is considered. The results reveal that when the Re increases, the total entropy also increases significantly (for Re varying from 25 to 400, the total entropy varied from 0.38 to 18922.67 W/K respectively) [7]. A numerical investigation of the entropy generation rate in a wavy sinusoidal channel with nanofluid (Cu-water) flow is considered. The effects of geometric and flow parameters, including the nanoparticle volume fraction ($0.01 < \phi < 0.05$), the Richardson number ($0.1 < Ri < 10$), the wave amplitude ($0.1 < \alpha < 0.3$) and the wavelength ratio ($1 < \lambda < 3$) have been studied. The results show that

for the studied Richardson number, the increase in the volume fraction of the nanoparticles causes the increase in the Nu. Also, as the Richardson number increases, the maximum rate of entropy generation decreases. The entropy generation turns out to be lowest for $\alpha = 0.2$ (optimal wave amplitude ratios $\lambda = 1$ and $\lambda = 2$). Similarly, minimum entropy generation occurs approximately at $\alpha = 0.1$ (for the wavelength ratio of $\lambda = 3$) [8]. A numerical study concerning the heat transfer characteristics of Al_2O_3-water nanofluid in a corrugated mini-channel with inlet pulsation is carried out. The results indicate that by using the nanoparticles under pulsed flow, a good thermal performance potential arises. Moreover, in the base fluid, the pulsed flow has the advantage of preventing the sedimentation of the nanoparticles. In addition, with increasing nanoparticle volume fraction and pulsation amplitude, heat transfer performance increases significantly, given in Akdag *et al.,* [9]. Ahmed *et al.,* [10] presented an experimental and numerical study of the S_iO_2-water nanofluid flow in different shapes: straight, trapezoidal and sinusoidal channels. The studies were carried out for Re varying from 400 to 4000 and volume fractions from 0 to 1%. The results showed that the heat transfer and the Nusselt number increase with increasing particle volume fraction at the expense of a pressure drop. In addition, the trapezoidal channel has the highest Nusselt number compared to the others. A numerical study to analyze the entropy generation of a turbulent flow with heat transfer, in corrugated helical tubes with Reynolds numbers varying from 10020 to 40060 and a constant temperature imposed on the wall, is carried out. The effects of ripple pitch and height on the flow as well as on the generation of entropy due to transfer and friction are presented. The results indicate that the local entropy of heat transfer improved with the increase of the secondary flux. Moreover, with the increase of the Reynolds number, the total and transfer entropy exhibits a linear growth while that due to friction exhibits exponential growth [11]. In a numerical study, the effect of SWCNT-water nanofluids and turbulent flow through a sinusoidal channel on thermal-hydraulic characteristics and entropy production was investigated. Reynolds number, pulsation frequency, phase shift and nanoparticle concentration were considered, and the results show a considerable effect of pulsation frequency and phase shift on heat transfer enhancement and entropy generation [12]. In an experimental and numerical study, the flow characteristics in a channel with rectangular ribs were investigated. The results show a Nusselt improvement of 1.9 to 2.4 times in the case of grooved channels compared with straight channels. This improvement is accompanied by a loss of pressure [13]. A numerical study of the heat transfer and flow of a nanofluid in a heat sink is carried out. The results show that Al_2O_3 nanofluid leads to a better heat transfer enhancement compared to water base fluid [14]. In a numerical study, the thermal performance of turbulent flow through an integrated circular pipe with and without dimples on a twisted ribbon was investigated. Numerical results show a variation of 4.15%, 3.89% and 7.65% in Re number compared with experimental data [15]. In a numerical study, the effect of the Al_2O_3/water nanofluid on the thermal-hydraulic performance of a serpentine tube is studied. Different volume flow rates and volume fractions were considered. The results showed an improvement in heat transfer for a high volume fraction and a high volume flow rate [16]. A numerical study of the effects of the cells on a heat exchanger concerning the thermal and hydraulic performances was brought back by using the nano hybrid Al_2O_3-Cu/water for various volume fractions. The results indicate an improvement heat exchange of 2.67 times for Re 5×10^3 as well as an increase in thermal efficiency with increasing volume fraction [17]. In a numerical investigation, the effect of dimpled surface on flow characteristics and heat transfer using Al_2O_3/water nanofluid was analyzed. The results indicate an improvement in thermal efficiency of 27% with the dimpled surface compared to that of a smooth channel and an increasing up to 32% of the thermal efficiency for a volume fraction of 4% is observed [18].

Our aim is to study the effect of Reynolds number (Re) on Nu, skin friction coefficient, pressure drop and PEC factor using nanofluid (Al_2O_3-Water). Irreversibility is taken into account by entropy generation due to transfer and friction.

2. Mathematical Formulation

The flow of a nanofluid (Al_2O_3-Water) considered in the present work, is stationary, two-dimensional, turbulent and with heat transfer. The following average equations governing such flow are:

2.1 Continuity Equation

$$\frac{\partial \overline{U}_i}{\partial x_i} = 0 \tag{1}$$

2.2 Momentum Equation

$$\frac{\partial}{\partial x_j}\left(\rho \overline{U}_j \overline{U}_i\right) = -\frac{\partial \overline{P}}{\partial x_i} + \frac{\partial}{\partial x_j}\left(\mu\left(\frac{\partial \overline{U}_i}{\partial x_j} + \frac{\partial \overline{U}_j}{\partial x_i}\right) - \overline{u'}_j \overline{u'}_i\right) \tag{2}$$

The sub-grid stress tensor contained in the last term of Eq. (2) is defined by:

$$\tau_{ij} \equiv \rho\left(\overline{U_i U_j} - \overline{U}_i \overline{U}_j\right) = -\mu_t \underbrace{\left[\frac{\partial \overline{U}_i}{\partial x_j} + \frac{\partial \overline{U}_j}{\partial x_i}\right]}_{2S_{ij}} + \frac{1}{3}\tau_{kk}\delta_{ij} \tag{3}$$

Based on Boussinesq's concept, its approximation gives:

$$\tau_{ij} = -\mu_t \underbrace{\left[\frac{\partial \overline{U}_i}{\partial x_j} + \frac{\partial \overline{U}_j}{\partial x_i}\right]}_{2S_{ij}} + \frac{1}{3}\tau_{kk}\delta_{ij} \tag{4}$$

S_{ij} is called the resolved scales strain rate tensor. From the Smagorinsky-Lilly model, we derive the sub-grid turbulent viscosity [19,20].

2.3 Energy Equation

$$\frac{\partial}{\partial x_j}\left(\rho C_p U_j \overline{T}\right) = -\frac{\partial}{\partial x_i} K\left(\frac{\partial \overline{T}}{\partial x_j} - \rho C_p \overline{u'}_j t'\right) \tag{5}$$

2.4 Turbulence Model

We use the (k-ε realizable) model It is a semi-empirical model based on Boussinesq's concept relating Reynolds stresses to mean strain rates using two transport equations which are the turbulent kinetic energy k (Eq. (6)) and its dissipation rate ε (Eq. (7)):

$$\frac{\partial}{\partial x_i}(\rho k U_i) = \frac{\partial}{\partial x_j}\left(\left(\mu + \frac{\mu_t}{\sigma_k}\right)\frac{\partial k}{\partial x_j}\right) + G_k - \rho\varepsilon \tag{6}$$

$$\frac{\partial}{\partial x_i}(\rho \varepsilon U_i) = \frac{\partial}{\partial x_j}\left(\left(\mu + \frac{\mu_t}{\sigma_\varepsilon}\right)\frac{\partial \varepsilon}{\partial x_j}\right) + C_{1\varepsilon} G_k \frac{\varepsilon}{k} - C_{2\varepsilon}\rho\frac{\varepsilon^2}{k} \tag{7}$$

Gk is the production of the kinetic turbulent energy defined as follows:

$$G_k = -\rho\overline{u_i u_j}\frac{\partial U_j}{\partial x_i} \tag{8}$$

In above equations, the turbulent Prandtl number and the empirical constants are:

$Prt = 0.85, C1k = 1, C2\varepsilon = 1.9, \sigma k = 1$ and $\sigma\varepsilon = 1.2$

2.5 Thermophysical Properties of Nanofluid (Al_2O_3/water)

To calculate the properties of the nanofluid, the following expressions are used:

Density

$$\boldsymbol{\rho}_{nf} = (1-\Phi)_f + \Phi\boldsymbol{\rho}_{np} \tag{9}$$

Heat capacity

$$(\boldsymbol{\rho}C_p)_{nf} = (1-\Phi)(\boldsymbol{\rho}C_p)_f + \Phi(\boldsymbol{\rho}C_p)_{np} \tag{10}$$

Dynamic viscosity

$$\mu_{nf} = \mu_f . [(1-34.87(d_p/d_f)^{-0.3}.\Phi^{1.03})]^{-1} \tag{11}$$

Where d_p= 30nm

Effective thermal conductivity

$$k_{eff} = k_{Brownian} + k_{static} \tag{12}$$

$$\text{Where } k_{static} = k_f(k_p+2k_f)-2\Phi(k_f - k_p) * (k_p+2k_f)-\Phi(k_f - k_p)^{-1} \tag{13}$$

$$k_{Brownian} = 5* 10^4 \beta\Phi\boldsymbol{\rho}_f C_p (\boldsymbol{\kappa}T/\boldsymbol{\rho}_p d_p)^{1/2} f(T,\Phi) \tag{14}$$

κ=1.381.10^{-23}J/K ;

For $1 \leq \Phi \leq 10$, β= 8.4407(100.Φ)$^{-1.07304}$ correlations of β [21]

The thermophysical properties of water and nanoparticules at T= 298 K, are summarized in Table 1 [22-24].

Table 1
Thermophysical properties of water and nanoparticules

Thermophysical properties	ρ (kg/m^3)	C_p (J/kg K)	k(W/m.K)	μ (kg/m.s)
Water	996.5	4181	0.613	0.001
Al_2O_3	3600	765	36	-

2.6 Entropy Generation

In turbulent fluid flow with heat transfer, the generation of total entropy is mainly due to temperature gradient (heat transfer), turbulent diffusion and dissipation, and fluid friction (viscous dissipation). All these effects occur mainly in the region close to the wall or a strongly sheared layer in which the variations of variables such as velocity and/or temperature are relatively high.

The generation of entropy caused locally by irreversibility can be considered as the sum of two contributions: that due to the difference in velocity S_{gf} (friction) and to the temperature difference S_{gt} (heat transfer). Beyond that, the global entropy generation is written as:

$$S_g = S_{gf} + S_{gt} \tag{15}$$

With S_{gt} : generation of entropy due to turbulent heat transfer given by the following equation:

$$s_{gt} = \frac{\alpha_{turbulent}(diffusivité\ turbulent)}{\alpha_{nf}(diffusivité\ )} \times \frac{K_{hnf}}{T_0^2}\left[\left(\frac{\partial T}{\partial x}\right)^2 + \left(\frac{\partial T}{\partial y}\right)^2 + \left(\frac{\partial T}{\partial z}\right)^2\right] \tag{16}$$

S_{gf} : the one that concerns the entropy generation due to fluid friction is given by:

$$s_{gf} = \frac{\rho_{nf}\varepsilon(\text{La } dissipation \text{ turbulente})}{T_0} + \frac{\mu_{nf}}{T_0}\left[2\left(\left(\frac{\partial u}{\partial x}\right)^2 + \left(\frac{\partial v}{\partial y}\right)^2\right) + \left(\frac{\partial u}{\partial y} + \frac{\partial v}{\partial x}\right)^2\right] \tag{17}$$

The S_{gt} to S_g ratio known as the Bejan number (Be) reflects the relative importance of the two main entropy generating mechanisms:

$$Be = \frac{s_{gt}}{Sg} \tag{18}$$

3. Numerical Solution Procedure

Solving the equations governing nanofluid flow in the corrugated channel is based on the finite volume method using the ANSYS-Fluent calculation code. The velocity-pressure coupling is taken into account by the SIMPLE algorithm. The second-order discretization scheme has been used to discretize the convective terms in the transport equation.

4. Numerical Resolution Method

In this work, the considered configuration is similar to that studied numerically by Ahmed *et al.,* [1]. It consists of two corrugated walls with a maximum of 12 mm (Hmax) and a minimum of 8 mm (Hmin). The lengths of the straight sections are respectively 800 and 200 mm upstream and downstream of the corrugated channel, which has a total length of 200 mm.

The wavelength and the amplitude are $Lw = 20mm$ and $a = 2mm$. In addition, a uniform heat flow is imposed on the corrugated walls (lower and upper) but the straight (upstream and downstream) parts are considered adiabatic, Figure 1.

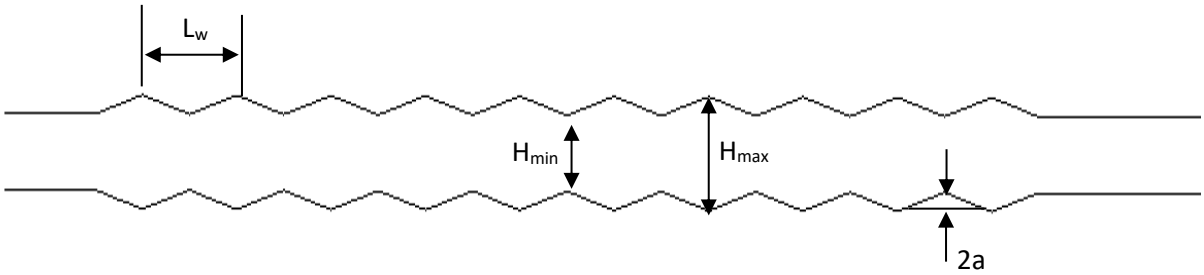

Fig. 1. Physical domain

4.1 Boundary Conditions

The inlet:
The inlet conditions are: a uniform velocity component in the x-direction (U_x) based on the Reynolds number, turbulent intensity of 1% is imposed and hydraulic diameter $D_h = H_{max} + H_{min}$

The walls:
The no-slip condition is imposed on the walls with the use of the standard wall function.

The outlet:
At the outlet of the domain, a constant atmospheric pressure is prescribed.

Different non dimensional terms will be used in this analysis. It consists of the Reynolds and the Nusselt number which are given by:

Reynolds number:

$$\mathrm{Re} = \frac{\rho \, u \, D_h}{\mu} \tag{19}$$

The hydraulic diameter D_h is calculated as:

$$D_h = \frac{4 \, S}{P_w} = 2H \tag{20}$$

Nusselt number:

The Nusselt number is defined as [25]:

$$Nu = \frac{hD_h}{K_{eff}} \tag{21}$$

The friction factor of the nanofluid, which is calculated as follows:

$$f = \frac{\Delta p.D_h}{L.\left(\frac{\rho_{nf}u_{in}{}^2}{2}\right)} \tag{22}$$

where ρ_{nf} represents the density and u the velocity of the nanofluid.

4.2 Mesh and Validation

In order to prove the independence of the mesh on the solution, six structured meshes were tested, Table 2.

Table 2
Tested structured meshes

	m1	m2	m3	m4	m5	m6
Cellules numbers	94732	108899	118041	133380	184647	236670

Figure 2(a) compares profiles of x-velocity at the position illustrated in the same figure ($x = 90$ mm from the inlet corrugation), also the Nu and skin friction coefficient for one corrugation are presented (Figure 2(b) and Figure 2(c), respectively). Since the obtained solutions were similar with all the grids, the results below have been discussed with the m2 grid.

Figure 3 Compares the variation of the Nusselt number as a function of the Reynolds number, with the numerical data of Ahmed *et al.,* [1]. The maximum error of the Nusselt is 13% at $e = 5000$. Thus, we noted a good agreement between the results.

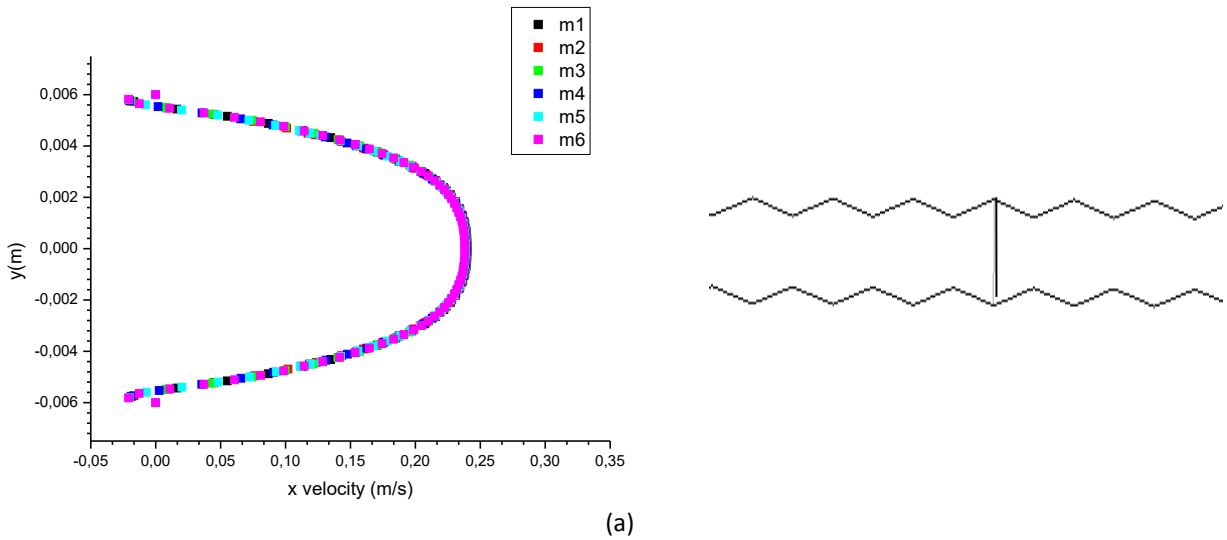

(a)

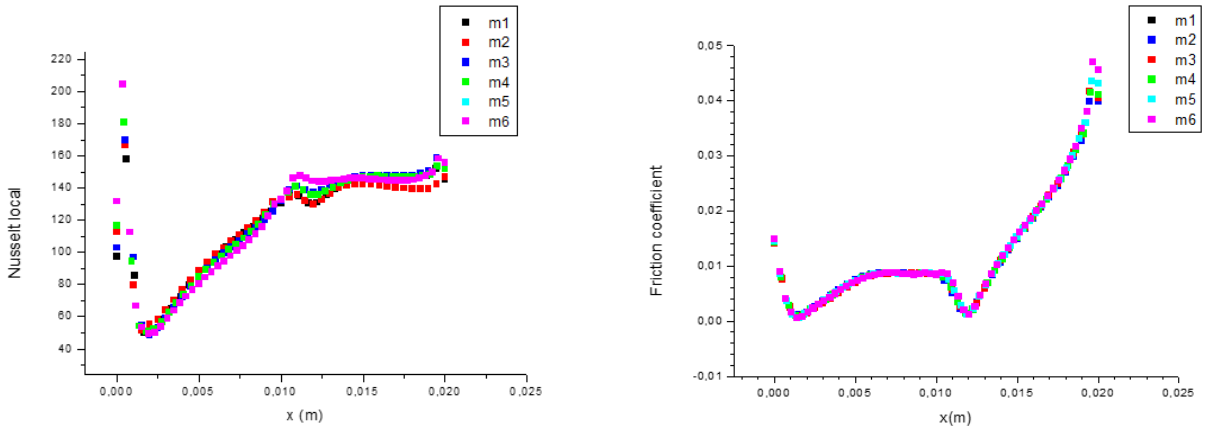

(b) (c)

Fig. 2. Grid independence test (a) x-velocity; (b) Local Nusselt number; (c) Skin friction coefficient

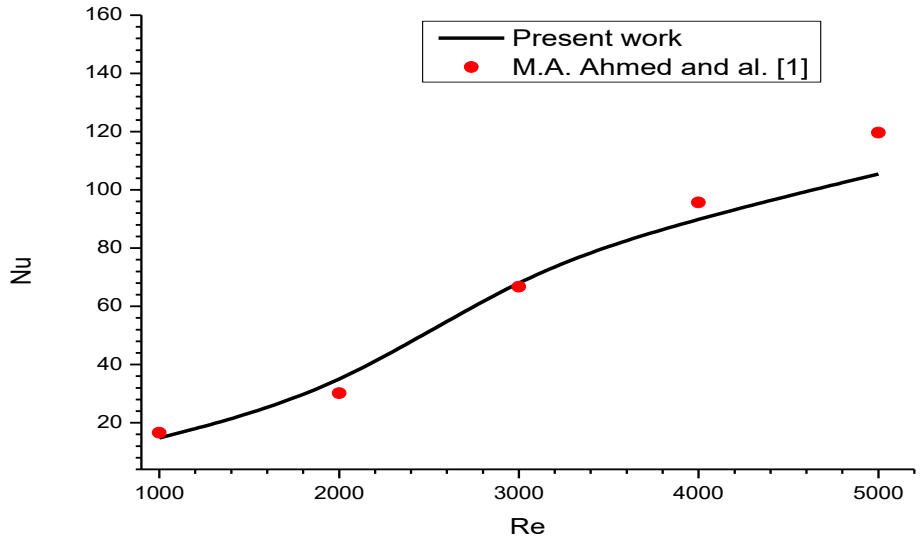

Fig. 3. Variations of Nusselt number versus the Reynolds number

5. Results and Discussion

Figure 4 illustrates the velocity contours, we can see that, with the increase in the Reynolds number, there is appearance of a central flow at significant velocity and which decreases as we approach the walls until it is canceled, which justifies the no-slip condition. We also note the appearance of recirculation zones in the divergent part of the channel, whose size varies proportionally with the increase of the Reynolds number.

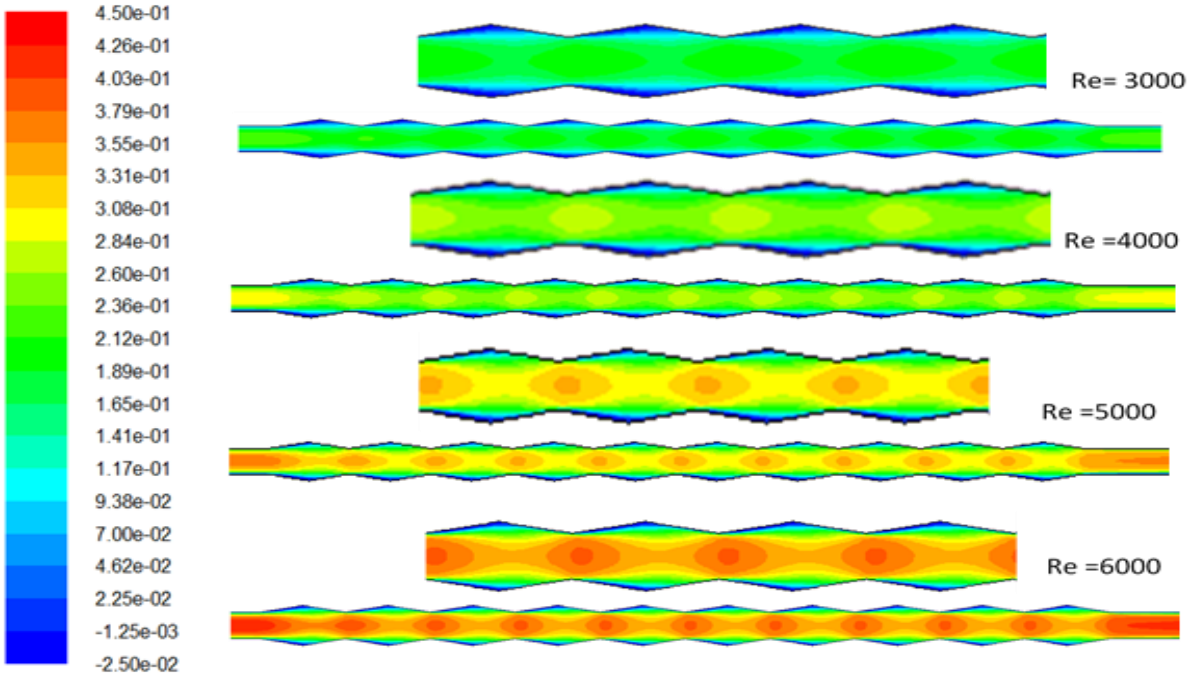

Fig. 4. Variations of x-velocity versus the Reynolds number

Figure 5 illustrates the static pressure contours, a decrease in pressure can clearly be seen where there has been an increase in velocity; phenomenon dictated by the momentum equation: all the kinetic energy is compensated by the pressure energy.

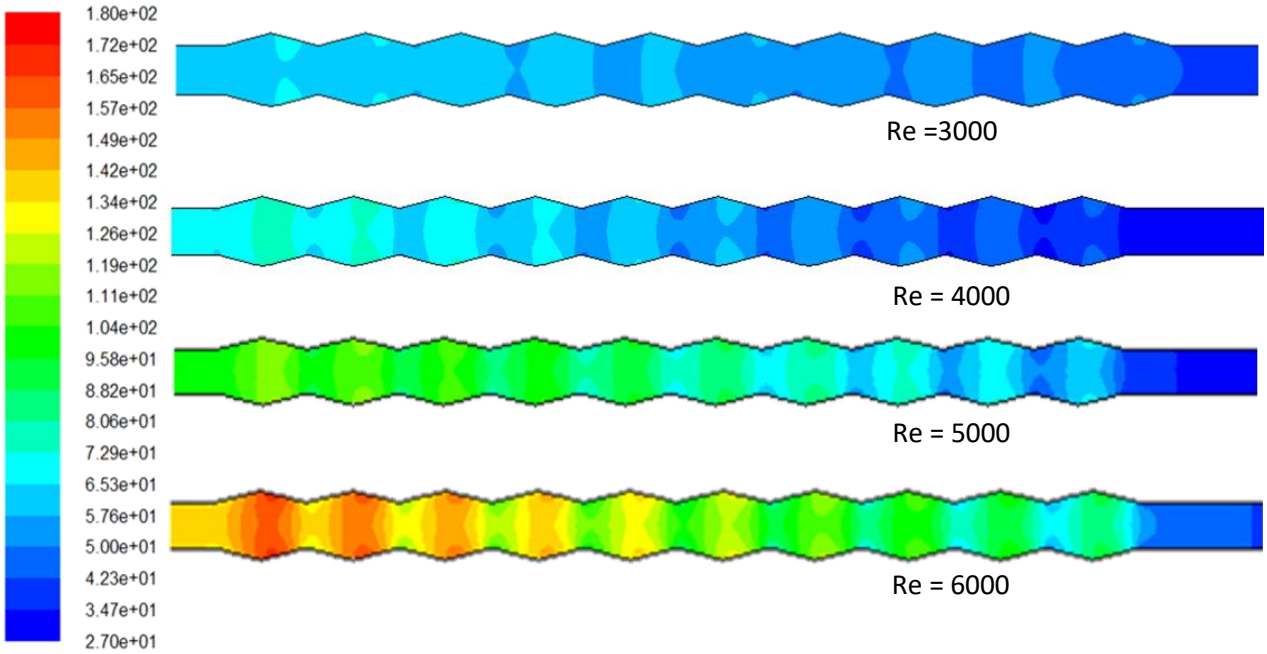

Fig. 5. Variations of pressure versus the Reynolds number

Figure 6(a) illustrates the variation of the average Nusselt number as a function of Reynolds number for water ($\Phi = 0\%$) and for the nanofluid Al_2O_3 / water ($\Phi = 3\%$). We can see that Nu increases with Re increment. The highest Nu values of the nanofluid are observed compared to those of water; this is explained by the increase in the thermal conductivity of the nanofluid by the Al_2O_3 nanoparticles. We also note that for the lower Re, the Nu number decreases and vice versa. We also

see in Figure 6(b), that the skin friction coefficient decreases with the increase of the Reynolds number for the two used fluids and it is clear that the friction factor is insensitive to the nanoparticles. On the Figure 6(c), it is noted that the pressure drop for the base fluid is less significant than that of the nanofluid, driven of course by its high viscosity. Moreover, the variation is monotonous, the pressure drops increase with the increase in the Reynolds number and therefore the nanofluid requires a high pumping power. The thermal-hydraulic performance factor of water at 0% is lower than that of the nanofluid at 3% for all values of the Reynolds number, Figure 6(d). This is due to its low thermal conductivity compared to that of the nanofluid. It is concluded that the addition of nanoparticles in the base fluid promotes heat transfer despite the increase in pressure drop.

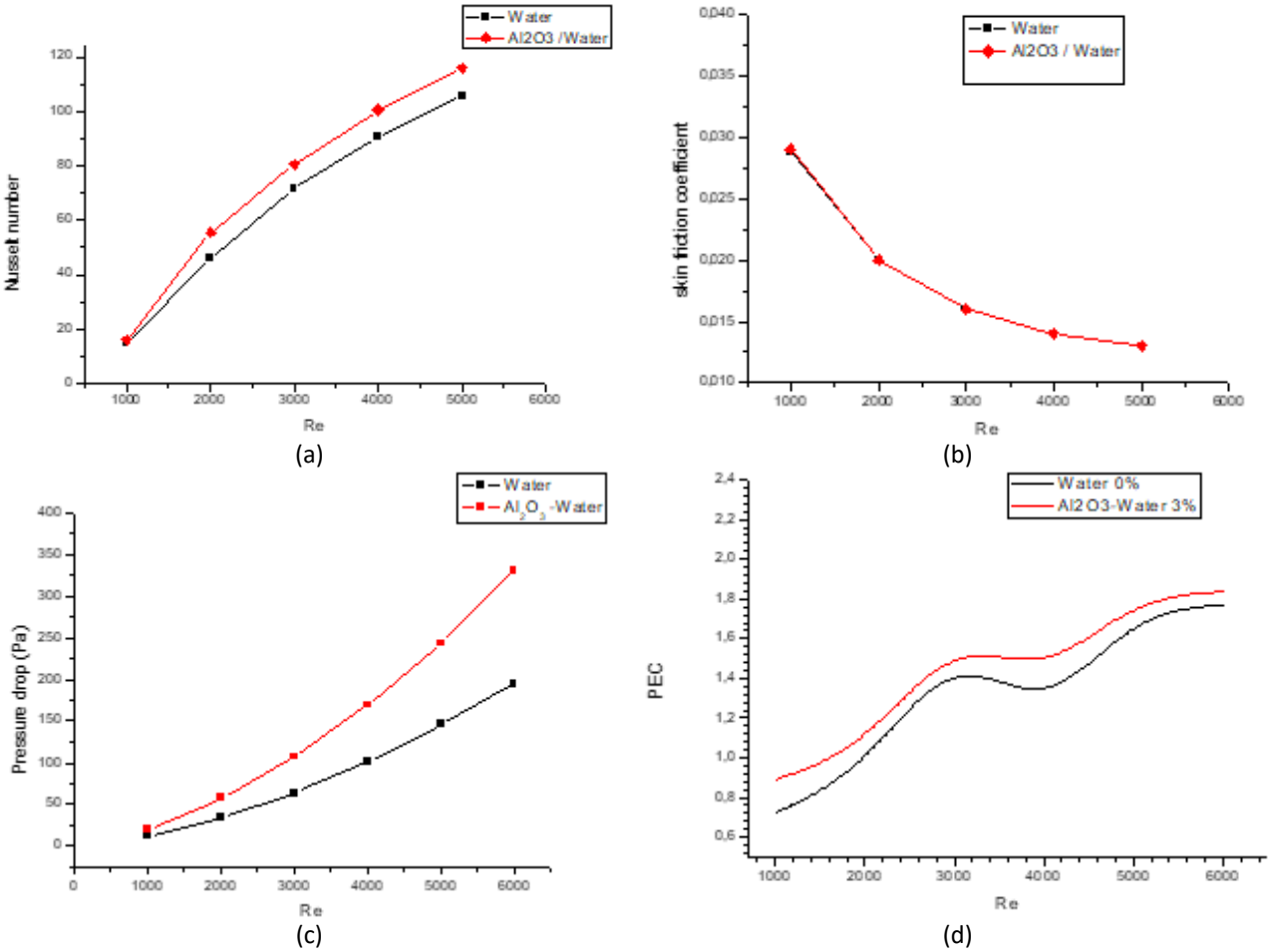

Fig. 6. Variation for different fluids on (a) Nusselt number; (b) skin friction coefficient; (c) pressure drop; (d) Thermal-hydraulic performance factor

The contours of the variation of the total entropy at different Reynolds number (Figure 7), show that the latter has a very weak effect on the contribution of the irreversibility but with respect to the central axis of the channel, the behavior is symmetrical. More or less significant values are noted at the level of the wall of the corrugated channel and which decrease as they move away towards the center due to the reduction in the temperature and velocity gradients.

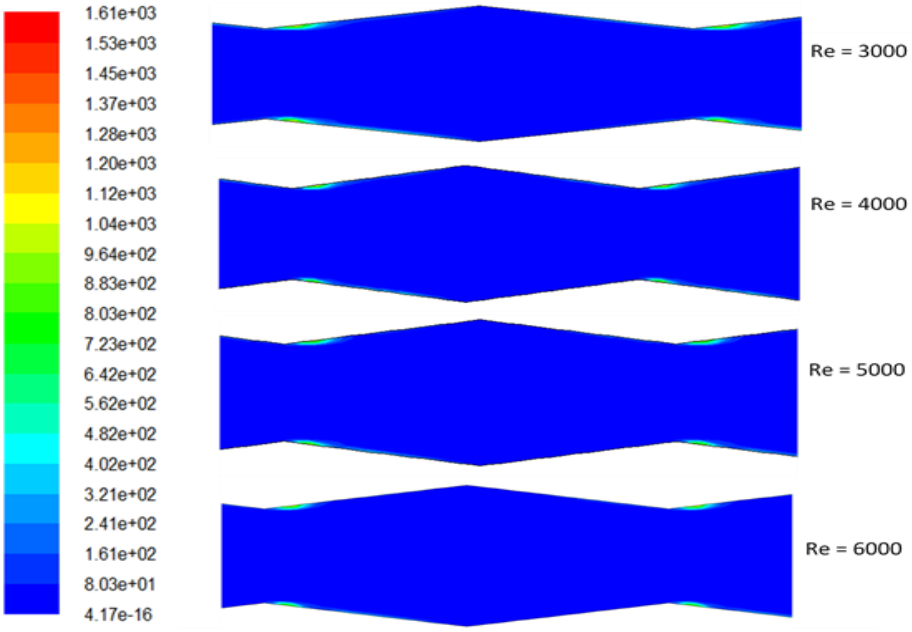

Fig. 7. Contours of total entropy versus the Reynolds number

On the Figure 8, the contours of the Bejan number reveal, that for different Reynolds numbers, the thermal entropy is the main production of the total entropy both at the level of the corrugated walls and in the whole domain, especially at Re=3000. Beyond this value, it is clearly seen, that the values of the Bejan number gradually decrease from the wall to the center of the channel, this means that the thermal production decreases and the production of friction entropy increases.

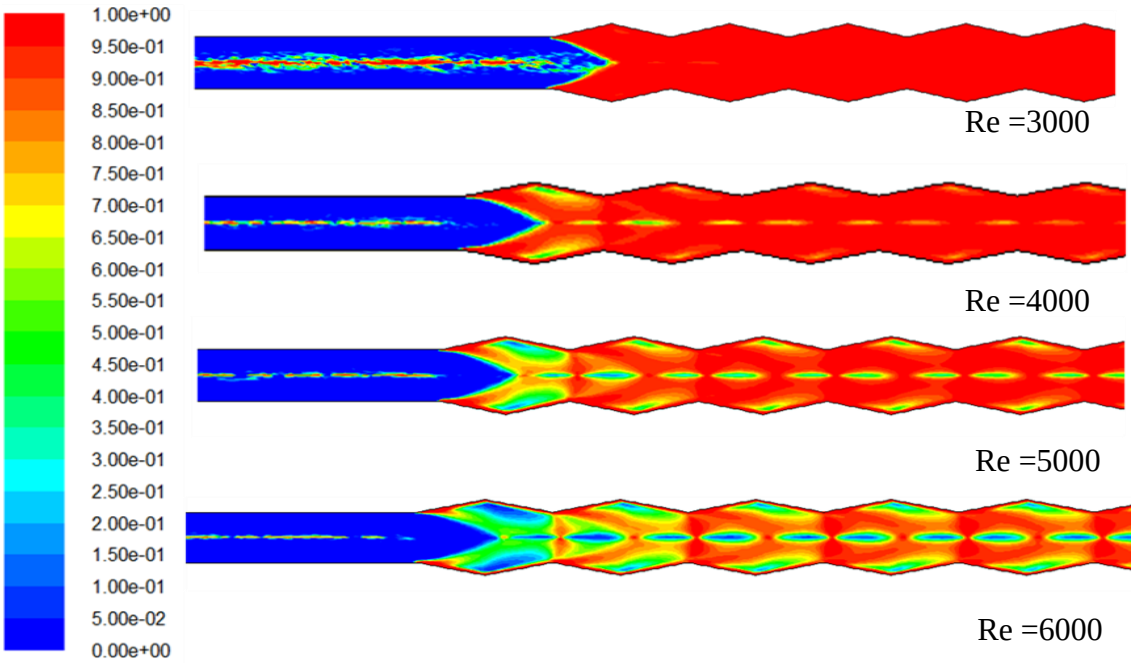

Fig. 8. Contours of Bejan number versus the Reynolds number

The effect of Re on thermal entropy in corrugated channel is shown in Figure 9(a). The result revealed that an increase in Reynolds leads a diminution of thermal entropy; this is due to the decrease of the temperature gradient. Figure 9(b) depicts the variation of friction entropy, it should be noted that the viscous entropy increases when Reynolds increases, this is caused by the rises of

the velocity gradient. The total entropy as function of Reynolds is illustrated in Figure 9(c). It can be seen that the total entropy decreases with the augmentation of Reynolds; we conclude that the contribution of thermal entropy is more important than that due to friction. In parallel, it is clearly seen that the Bejan number decreases with the increase in the Reynolds number, Figure 9(d).

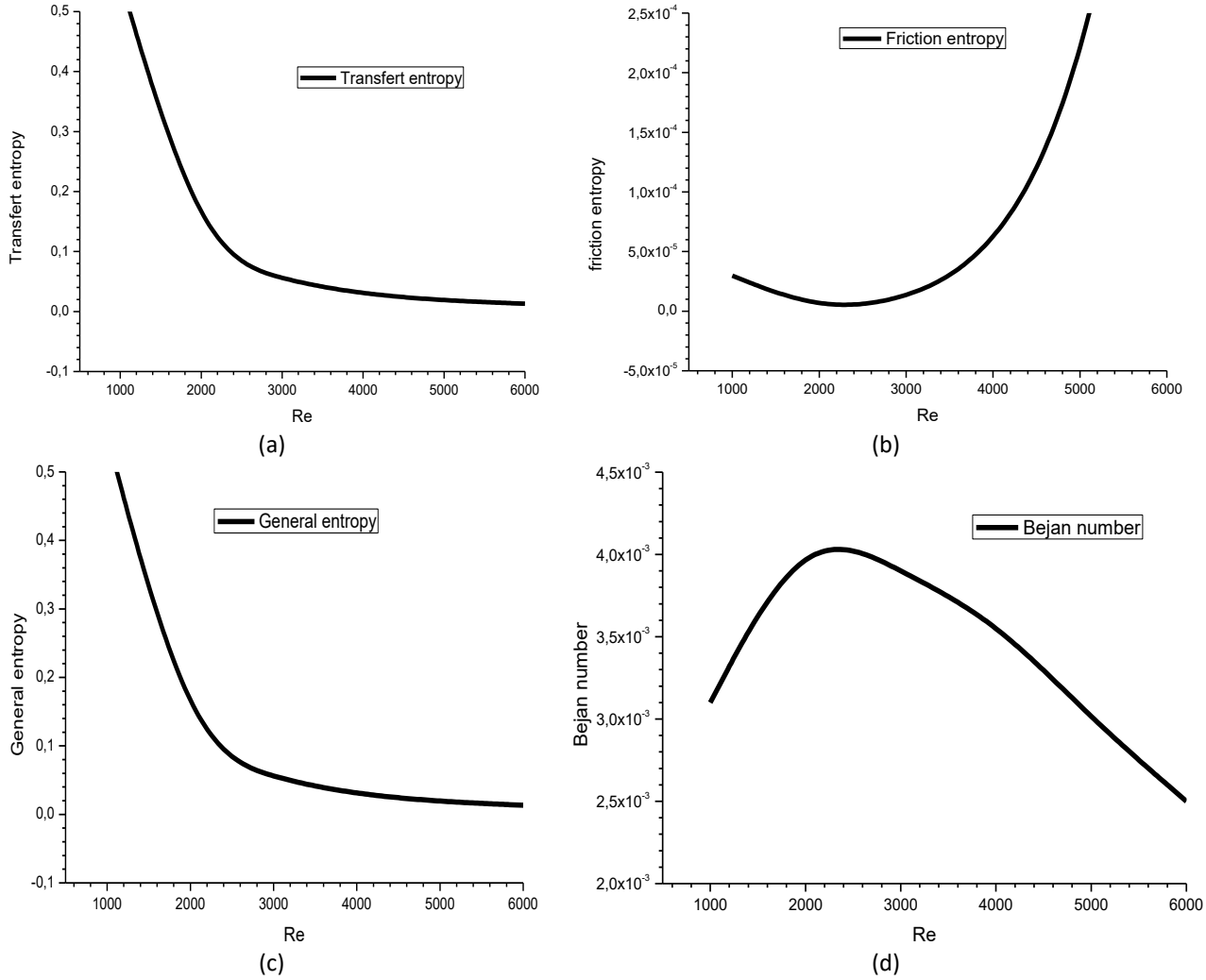

Fig. 9. Effect of Reynolds number on (a) Thermal entropy; (b) Friction entropy; (c) Total entropy; (d) Bejan number

6. Conclusions

The numerical study of a simplified geometric configuration represented by a corrugated channel, allowed us a better understanding of the behavior of the two-dimensional flow of nanofluid, using the ANSYS Fluent code.
The simulation results can be summarized as:

i. The comparison of the shapes of the numerical obtained results with those of Ahmed *et al.,* [1] showed a rather acceptable agreement.
ii. The increase in the Reynolds number leads to an increase in the average Nusselt and a decrease in the coefficient of friction.
iii. The use of nanofluid Al_2O_3/water gives better heat transfer than pure water.

iv. The central flow with maximum velocity at the level of the channel axis and accompanied by a pressure drop, increases with the increase in the Reynolds number.

v. The transfer entropy generated in the fluid crossing the channel as well as the Bejan number decrease with the increase of the Reynolds, while that of the friction increases, this is explained by the fact that it is the dissipation of kinetic turbulent energy due to the effect of viscosity which most degrades the useful energy in the fluid and it's friction by turbulence which generates the most entropy.

vi. The maximum heat transfer and low production rate of entropy generation is obtained at the maximum and the minimum values of the Reynolds number, respectively.

References

[1] Ahmed, M. A., Mohd Zamri Yusoff, Khai Ching Ng, and N. H. Shuaib. "Numerical investigations on the turbulent forced convection of nanofluids flow in a triangular-corrugated channel." *Case Studies in Thermal Engineering* 6 (2015): 212-225. https://doi.org/10.1016/j.csite.2015.10.002

[2] Manca, Oronzio, Sergio Nardini, and Daniele Ricci. "A numerical study of nanofluid forced convection in ribbed channels." *Applied Thermal Engineering* 37 (2012): 280-292. https://doi.org/10.1016/j.applthermaleng.2011.11.030

[3] Chen, Xin, Huaizhi Han, Kwan-Soo Lee, Bingxi Li, and Yaning Zhang. "Turbulent heat transfer enhancement in a heat exchanger using asymmetrical outward convex corrugated tubes." *Nuclear Engineering and Design* 350 (2019): 78-89. https://doi.org/10.1016/j.nucengdes.2019.05.001

[4] Ajeel, Raheem K., W. S-I. W. Salim, and Khalid Hasnan. "Experimental and numerical investigations of convection heat transfer in corrugated channels using alumina nanofluid under a turbulent flow regime." *Chemical Engineering Research and Design* 148 (2019): 202-217. https://doi.org/10.1016/j.cherd.2019.06.003

[5] Aminian, Ehsan, Hesam Moghadasi, Hamid Saffari, and Amir Mirza Gheitaghy. "Investigation of forced convection enhancement and entropy generation of nanofluid flow through a corrugated minichannel filled with a porous media." *Entropy* 22, no. 9 (2020): 1008. https://doi.org/10.3390/e22091008

[6] Yang, Xianglong, and Lei Yang. "Numerical Study of Entropy Generation in Fully Developed Turbulent Circular Tube Flow Using an Elliptic Blending Turbulence Model." *Entropy* 24, no. 2 (2022): 295. https://doi.org/10.3390/e24020295

[7] Bahaidarah, Haitham M. S. "Entropy generation during fluid flow in sharp edge wavy channels with horizontal pitch." *Advances in Mechanical Engineering* 8, no. 8 (2016): 1687814016660929. https://doi.org/10.1177/1687814016660929

[8] Dormohammadi, Reza, Mahmood Farzaneh-Gord, Amir Ebrahimi-Moghadam, and Mohammad Hossein Ahmadi. "Heat transfer and entropy generation of the nanofluid flow inside sinusoidal wavy channels." *Journal of Molecular Liquids* 269 (2018): 229-240. https://doi.org/10.1016/j.molliq.2018.07.119

[9] Akdag, Unal, Selma Akcay, and Dogan Demiral. "Heat transfer enhancement with laminar pulsating nanofluid flow in a wavy channel." *International Communications in Heat and Mass Transfer* 59 (2014): 17-23. https://doi.org/10.1016/j.icheatmasstransfer.2014.10.008

[10] Ahmed, M. A., Mohd Zamri Yusoff, Khai Ching Ng, and N. H. Shuaib. "Numerical and experimental investigations on the heat transfer enhancement in corrugated channels using SiO_2-water nanofluid." *Case Studies in Thermal Engineering* 6 (2015): 77-92. https://doi.org/10.1016/j.csite.2015.07.003

[11] Wang, Wei, Yaning Zhang, Jian Liu, Zan Wu, Bingxi Li, and Bengt Sundén. "Entropy generation analysis of fully-developed turbulent heat transfer flow in inward helically corrugated tubes." *Numerical Heat Transfer, Part A: Applications* 73, no. 11 (2018): 788-805. https://doi.org/10.1080/10407782.2018.1459137

[12] Hamzah, Hudhaifa, and Besir Sahin. "Analysis of SWCNT-water nanofluid flow in wavy channel under turbulent pulsating conditions: Investigation of homogeneous and discrete phase models." *International Journal of Thermal Sciences* 184 (2023): 108011. https://doi.org/10.1016/j.ijthermalsci.2022.108011

[13] Zontul, Harun, Hudhaifah Hamzah, Nazım Kurtulmuş, and Beşir Şahin. "Investigation of convective heat transfer and flow hydrodynamics in rectangular grooved channels." *International Communications in Heat and Mass Transfer* 126 (2021): 105366. https://doi.org/10.1016/j.icheatmasstransfer.2021.105366

[14] Jowsey, Mohamad Hafzan Mohamad, Natrah Kamaruzaman, and Mohsin Mohd Sies. "Heat and Flow Profile of Nanofluid Flow Inside Multilayer Microchannel Heat Sink." *Journal of Advanced Research in Micro and Nano Engineering* 4, no. 1 (2021): 1-9.

[15] Fekadu, Birlie, H. V. Harish, and K. Manjunath. "Numerical Studies on Thermo-Hydraulic Characteristics of Turbulent Flow in a Tube with a Regularly Spaced Dimple on Twisted Tape." *CFD Letters* 13, no. 8 (2021): 20-31. https://doi.org/10.37934/cfdl.13.8.2031

[16] Awais, M., M. Saad, Hamza Ayaz, M. M. Ehsan, and Arafat A. Bhuiyan. "Computational assessment of Nano-particulate (Al_2O_3/Water) utilization for enhancement of heat transfer with varying straight section lengths in a serpentine tube heat exchanger." *Thermal Science and Engineering Progress* 20 (2020): 100521. https://doi.org/10.1016/j.tsep.2020.100521

[17] Ratul, Raditun E., Farid Ahmed, Syed Alam, Md Rezwanul Karim, and Arafat A. Bhuiyan. "Numerical study of turbulent flow and heat transfer in a novel design of serpentine channel coupled with D-shaped jaggedness using hybrid nanofluid." *Alexandria Engineering Journal* 68 (2023): 647-663. https://doi.org/10.1016/j.aej.2023.01.061

[18] Ahmed, Farid, Md Atrehar Abir, A. S. M. Redwan, Arafat A. Bhuiyan, and A. S. Mollah. "The impact of D-shaped jaggedness on heat transfer enhancement technique using Al_2O_3 based nanoparticles." *International Journal of Thermofluids* 10 (2021): 100069. https://doi.org/10.1016/j.ijft.2021.100069

[19] Smagorinsky, Joseph. "General circulation experiments with the primitive equations: I. The basic experiment." *Monthly Weather Review* 91, no. 3 (1963): 99-164. https://doi.org/10.1175/1520-0493(1963)091<0099:GCEWTP>2.3.CO;2

[20] Lilly, Douglas K. "A proposed modification of the Germano subgrid-scale closure method." *Physics of Fluids A: Fluid Dynamics* 4, no. 3 (1992): 633-635. https://doi.org/10.1063/1.858280

[21] Vajjha, Ravikanth S., and Debendra K. Das. "A review and analysis on influence of temperature and concentration of nanofluids on thermophysical properties, heat transfer and pumping power." *International Journal of Heat and Mass Transfer* 55, no. 15-16 (2012): 4063-4078. https://doi.org/10.1016/j.ijheatmasstransfer.2012.03.048

[22] Pak, Bock Choon, and Young I. Cho. "Hydrodynamic and heat transfer study of dispersed fluids with submicron metallic oxide particles." *Experimental Heat Transfer an International Journal* 11, no. 2 (1998): 151-170. https://doi.org/10.1080/08916159808946559

[23] Xuan, Yimin, and Wilfried Roetzel. "Conceptions for heat transfer correlation of nanofluids." *International Journal of Heat and Mass Transfer* 43, no. 19 (2000): 3701-3707. https://doi.org/10.1016/S0017-9310(99)00369-5

[24] Corcione, Massimo. "Empirical correlating equations for predicting the effective thermal conductivity and dynamic viscosity of nanofluids." *Energy Conversion and Management* 52, no. 1 (2011): 789-793. https://doi.org/10.1016/j.enconman.2010.06.072

[25] Kalteh, Mohammad, Abbas Abbassi, Majid Saffar-Avval, and Jens Harting. "Eulerian-Eulerian two-phase numerical simulation of nanofluid laminar forced convection in a microchannel." *International Journal of Heat and Fluid Flow* 32, no. 1 (2011): 107-116. https://doi.org/10.1016/j.ijheatfluidflow.2010.08.001